https://doi.org/10.5194/egusphere-2026-2179
Preprint. Discussion started: 2 June 2026

Effects of snow redistribution parameterization on simulated snow thickness validated by MOSAiC observations

Fengguan Gu[1] Changwei Liu[1] Bo Han[1] Qinghua Yang[1] Jiping Liu[1*]

1. School of Atmospheric Sciences, Sun Yat-sen University, and Southern Marine Science and Engineering Guangdong Laboratory (Zhuhai), Zhuhai, China

Corresponding authors: Jiping Liu (liujp63@mail.sysu.edu.cn)

Abstract

Snow plays a critical role in the mass and energy balance of sea ice through its insulating properties and high albedo. Based on observations from the Multidisciplinary Drifting Observatory for the Study of Arctic Climate (MOSAiC) campaign, we assess the influence of snow redistribution on snow thickness simulations using the Icepack column model. Our results show that, without snow redistribution, snow thickness is overestimated in winter and spring. The bulk redistribution scheme slightly reduces snow accumulation, while the blowing snow scheme (snwITDrdg) further increases agreement with observations but still shows biases during snowfall events. Sensitivity experiments indicate that setting the ratio of snow mass on ridges to that on level ice to 4 in the bulk scheme yields the best agreement with snow observations (MAE = 6.2 mm). In the snwITDrdg scheme, the snow erosion coefficient is treated as an effective tuning parameter. When observed sea ice concentration is prescribed, setting the snow erosion coefficient to 2.4×10^{-5} produces simulated accumulated snow loss to leads consistent with observations and improves the simulated snow thickness (MAE = 6.4 mm). This study provides new insights into snow thickness simulation and the parameterization of snow

https://doi.org/10.5194/egusphere-2026-2179
Preprint. Discussion started: 2 June 2026

redistribution, offering valuable guidance for improving Arctic snow thickness modeling.

1. Introduction

Snow cover on sea ice exerts a critical influence on the mass and energy balance of the ice through its high albedo and strong insulating properties (Callaghan et al., 2011; Maykut & Untersteiner, 1971; Webster et al., 2018). Its impact, however, is multifaceted and seasonally variable. In winter, snow insulates sea ice from the atmosphere, suppressing ice growth. In summer, thick snow preserves high albedo and resists melting, while thin snow is more prone to forming melt ponds, enhancing solar energy absorption (Eicken et al., 2004; Perovich et al., 2002; Polashenski et al., 2012). Snow accumulation can also lead to flooding and the formation of snow-ice, a process well documented in Antarctic first-year ice (Jeffries et al., 2001; Leppäranta, 1983; Maksym & Jeffries, 2000; Massom et al., 2001), and increasingly reported in the Arctic with the ongoing thinning of sea ice (Kwok, 2018; Granskog et al., 2017; Merkouriadi et al., 2017, 2020). Additionally, summer snow meltwater can percolate into the snowpack and refreeze as superimposed ice, further contributing to sea ice mass (Cheng et al., 2003; Eicken et al., 2004; Wang et al., 2015). Therefore, an accurate representation of snow thickness is essential for improving sea ice modeling and evolution.

In snow thickness simulations, snowfall is the primary factor influencing the spatial distribution of snow thickness (Wagner et al., 2022). In addition, snow redistribution parameterizations also influence the simulated snow thickness. The Icepack 1.3.2 sea ice column model includes two snow redistribution processes: bulk redistribution and snwITDrdg redistribution. The bulk snow redistribution parameterization is based on previous observational studies (Sturm et al., 2002) and assumes that approximately

https://doi.org/10.5194/egusphere-2026-2179
Preprint. Discussion started: 2 June 2026

30% of snowfall is effectively lost due to ice surface heterogeneity, such as leads and ridges. This approach reduces the effective snowfall reaching the ice surface, thereby decreasing the simulated snow thickness (Hunke et al., 2022). Beyond bulk redistribution, snwITDrdg redistribution is a crucial physical process that determines the spatial distribution of snow thickness (Olivier Lecomte et al., 2015; Leonard & Maksym, 2011; Liston et al., 2020). In snwITDrdg redistribution, strong winds can lift snow particles from the surface, and a portion of these suspended particles fall into open leads (Olivier Lecomte et al., 2015; Leonard & Maksym, 2011; Petty et al., 2018; Van den Broeke et al., 2004), while the remaining particles are redistributed on the snow surface, thereby altering the spatial distribution of snow thickness and affecting the mass and energy balance of the snow (Luo & Zhang, 2022). Blowing snow can also facilitate the sublimation of suspended snow particles (Déry & Yau, 2002; Liston et al., 2020), and studies have shown that under the same atmospheric conditions, the sublimation rate of blowing snow is two orders of magnitude higher than that of a stationary snow surface (Schmidt, 1982). In the Southern Ocean, about half of the snowfall eventually falls into open leads (Leonard & Maksym, 2011). During the MOSAiC expedition, observations indicate that under typical winter conditions, leads have a minimal impact on the snow mass balance, but when snowfall occurs alongside strong winds and high temperatures, 65%-100% of the recent snowfall can fall into open leads (Clemens Sewall et al., 2023), as strong winds promote snow redistribution and higher temperatures prevent rapid lead refreezing. Parameterizations of snow redistribution by wind have been applied in climate models (Olivier Lecomte et al., 2015) and data assimilation products (Petty et al., 2018). However, these approaches typically rely on simplified assumptions or tuning parameters and have not been extensively evaluated against detailed observations.

The Icepack 1.3.2 sea ice column model incorporates a parameterization for snow redistribution (Lecomte et al., 2013), yet many of its empirical coefficients have not been updated with recent observations or systematically validated. Previous studies

https://doi.org/10.5194/egusphere-2026-2179
Preprint. Discussion started: 2 June 2026

using the Icepack model have examined the performance of snow redistribution processes in simulating snow thickness (Hao et al., 2025; Zhao et al., 2025). However, the lack of accurate snowfall observations and measurements of snow blown into open leads introduces uncertainty in snow thickness simulations. In this study, we use atmospheic, oceanic and sea ice observations from the MOSAiC expedition to evaluate Icepack's snow redistribution, examine its impact on simulated Arctic snow thickness and explore avenues for further optimization. Section 2 describes the data and methods. Section 3 presents the performance of different snow redistribution processes on snow thickness simulation (3.1) and proposes improvements to the snow redistribution parameterization (3.2). Section 4 provides conclusions and discussions.

2. Data and methods

2.1 Icepack

The Icepack single-column model is a state-of-the-art numerical model managed by the CICE consortium. It contains physical processes that affect sea ice thickness within a single grid cell without reference to adjacent grid cells. Subgrid ice classes are described by dividing the ice area fraction into discrete thickness categories within each grid cell. The model solves a set of equations that represent ice dynamics, thermodynamics, and mechanical redistribution (ridging). This study used Icepack version 1.3.2 (Hunke et al., 2022). The observed atmospheric and oceanic forcing data are used as input for model simulations. The focus is on the effects of snow redistribution parameterization on snow thickness simulation. The model is initialized with observed ice thickness and snow thickness. The model settings, physical parameterizations are the same as those of previous studies (Gu et al., 2022). Following Clemens-Sewall et al. (2022), the Icepack ice thickness distribution is divided into 15 categories to more accurately represent the distribution of snow thickness.

https://doi.org/10.5194/egusphere-2026-2179
Preprint. Discussion started: 2 June 2026

2.2 Observational data

For this study, we used a comprehensive set of observational data encompassing atmospheric, oceanic, sea ice and snow thickness measurements collected during the MOSAiC expedition, which took place from October 2019 to September 2020. All observations were obtained within an area of approximately 15 km (Bliss et al., 2023). The atmospheric data included the Met City monitoring station and three Atmospheric Surface Flux Stations (Shupe et al., 2022). We used averaged atmospheric data from Met City and three ASFS sites as forcing for Icepack. The variables include downward shortwave and longwave radiation, 2 m air temperature, 2 m specific humidity, and 10 m wind speed. The ASFS 2 m wind speed was extrapolated to 10 m using a power-law relationship with a sea-ice surface roughness length of 1.0×10^{-3} m, following the ECMWF-IFS model (Ruti et al., 2008). Oceanographic data comprised 10-meter sea temperature and salinity measurements from eight Conductivity, Temperature, and Depth (CTD) buoys, as well as 3-meter sea temperature, salinity, and current velocity data from four autonomous ocean flux buoys. The observed sea temperature, salinity were prescribed as time-dependent external forcing in the Icepack simulations. The observed current velocities were used to calculate the friction velocity, which is used to estimate ocean–ice heat exchange. All ocean observations are confined within the mixed layer depth (Rabe et al., 2022). The spatially averaged values of these observations are used as oceanic forcing to simulate snow thickness. The ice opening and closing rates (s^{-1}) are derived from SAR-based sea ice divergence in the Transpolar Drift during MOSAiC 2019/2020 (von Albedyll, 2024), following the method described by Bitz (n.d.). In addition, precipitation data from the present weather detector (PWD) on the deck of the Polarstern and from the ERA5 reanalysis (Wagner et al., 2022) were used. Observed snow thickness was obtained from the Snow and Ice Mass Balance (SIMBA) array (Lei et al., 2022). In this study, 7 buoys were selected based on their operational periods, and their mean

https://doi.org/10.5194/egusphere-2026-2179
Preprint. Discussion started: 2 June 2026

snow thickness and mean ice thickness were used to evaluate the simulated snow and ice thickness. Snow observations were converted to snow water equivalent (SWE) using fitted SnowMicroPen (SMP) density–SWE relationships (Wagner et al., 2022). Daily sea ice concentration data were obtained from the Advanced Microwave Scanning Radiometer 2 (AMSR2) using the Arctic Sea Ice (ASI) algorithm (Spreen et al., 2008) developed at the University of Bremen, at a spatial resolution of 3.125 km.

2.3 Snow redistribution physical process

Snow acts as an insulating layer between the atmosphere and sea ice, altering the albedo of the sea ice surface, thereby exerting a strong influence on the simulated sea ice mass and energy balance. In Icepack, snow mass evolves through snowfall, melting, sublimation, snow-ice formation, and wind-driven processes (Hunke et al., 2022).

Icepack includes two snow redistribution processes: bulk redistribution and snwITDrdg redistribution. In the bulk redistribution scheme, based on SHEBA observational data, Icepack assumes that snow thickness in proximity of ice ridges is approximately 30% greater than that on level ice. To account for this preferential accumulation on ridges, Icepack effectively reduces the fraction of snowfall contributing to snow accumulation on level ice, which leads to a decrease in the simulated snow thickness over these areas (Hunke et al., 2022). The reduced snowfall represents snow that is instantaneously redistributed and lost to the ocean through leads. Mathematically, the amount of snow entering the leads is given by:

$$s_f^{'} = s_f\,[a_{lvl}\,(\frac{p}{1+p})]$$

where s_f is the snowfall rate, a_{lvl} is the area of the layer ice within a grid cell, and p is the ratio of snow depth on ridges to that on layer ice.

https://doi.org/10.5194/egusphere-2026-2179
Preprint. Discussion started: 2 June 2026

In the processes of snwITDrdg redistribution, the erosion rate of the snow is expressed as:

$$\Phi^{T}_{local} = \left(\frac{\partial m}{\partial t}\right)_{erosion} = -\frac{\gamma}{\sigma ITD}(V - V^{*})\frac{\rho_{max} - \rho_{s}}{\rho_{max}} ,$$

where ρ_{max} and ρ_s are the maximum snow density and the effective snow density in Icepack, respectively. The value of ρ_{max} is set to 400 kg m^{-3} (Macfarlane et al., 2023). After erosion begins, snow particles start to suspend when the instantaneous wind speed V exceeds a threshold (V^{*}). σITD is the standard deviation of the sea ice thickness distribution within a grid cell (Hunke et al., 2022). γ is a tuning coefficient that modulates the snow erosion rate, set to 1×10^{-5} kg m^{-2} (Lecomte et al., 2015). In Icepack, the default snow density is set to 330 kg/m^3 The threshold wind speed for snow erosion is calculated based on this snow density following Lecomte et al. (2013). Icepack further accounts for wind-induced compaction of the upper snow layer into denser wind slabs, which limits subsequent snow erosion; details are provided in the Icepack technical documentation.

The remaining suspended snow particles are redistributed over the ice surface as:

$$\Phi^{R}_{local}\Delta t = a_i(1 - f)\Phi^{T}_{local}\Delta t$$

Where f represents the fraction of suspended snow particles lost within the leads (Lecomte et al., 2013):

$$f = (1 - a_i)\exp\left(\frac{\sigma ITD}{\sigma ref}\right)$$

Where σref=1 m, and a_i is the area of the ice within a grid cell.

https://doi.org/10.5194/egusphere-2026-2179
Preprint. Discussion started: 2 June 2026

Snow loss to leads therefore occurs both through direct snowfall onto open water when sea ice concentration is below unity and through wind-driven snow erosion when wind speed exceeds a threshold. Icepack assumes local conservation of snow mass during blowing-snow redistribution, neglecting non-local transport between grid cells (Lecomte et al., 2015). Snow redistribution directly modifies the snow thickness associated with each ice thickness category and therefore affects the thermodynamic evolution of snow and ice. However, because Icepack assumes a uniform snow thickness within each category, subgrid-scale spatial heterogeneity in snow redistribution is not explicitly resolved. Although snow thickness directly affects the thermodynamic mass balance, the effects of its spatial variability are primarily represented through the surface radiation scheme, which responds to changes in effective surface fractions (Hunke et al., 2022).

3. Results

3.1 Snow Thickness Simulation Based on Different Snow Redistribution Processes

To simulate snow thickness during the MOSAiC period, we force the Icepack sea ice column model with mean atmospheric and oceanic observations. Given the critical role of precipitation in snow accumulation, we follow Wagner et al. (2022), who reported that actual precipitation lies between PWD and ERA5 estimates. We use the average of these two datasets, which is consistent with the observed range reported in their study, yielding a cumulative total of 91 mm from October 31, 2019, to April 26, 2020, within the observed range of 72–107 mm.

https://doi.org/10.5194/egusphere-2026-2179
Preprint. Discussion started: 2 June 2026

196 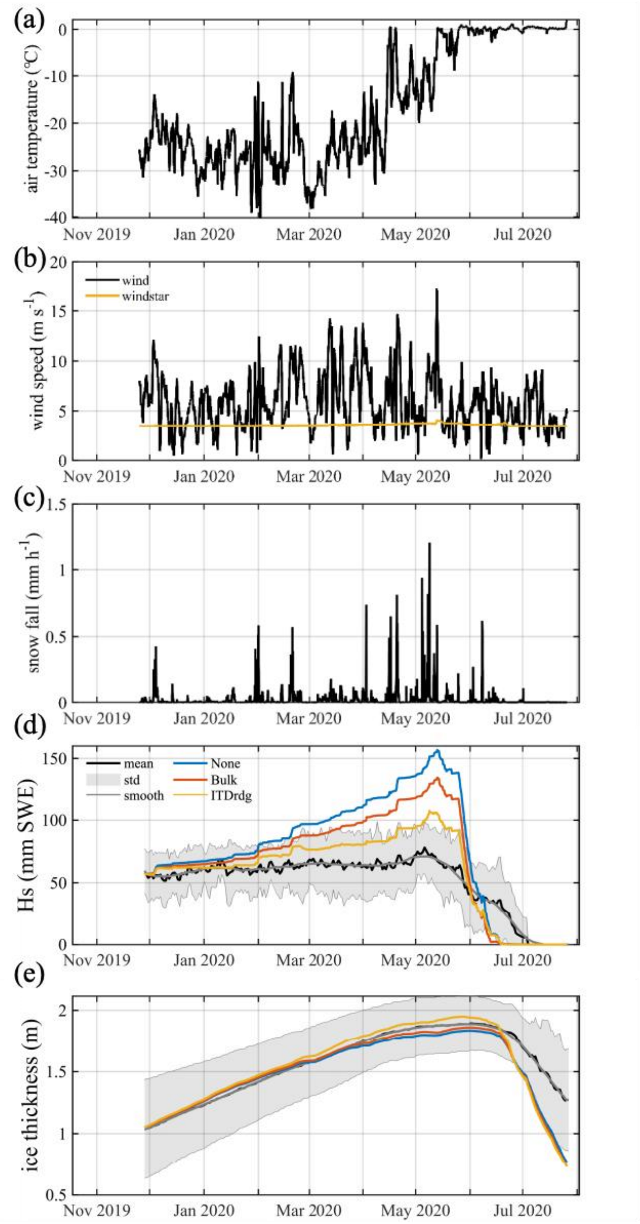

197 Figure 1. Time series simulation of (a) 2m air temperature, (b) 10m wind speed, (c)
198 snowfall, (d) snow thickness, and (e) ice thickness. The black line represents the
199 observation, and the yellow line in (b) represents the wind speed threshold (windstar)
200 for snow erosion and suspension in the snwITDrdg scheme. In (d) and (e), the thick
201 black line and grey shading represent the multi-site mean observations and their

standard deviation, respectively, while the thin black line indicates the 20-day moving average of the mean observations. The blue, red, and yellow lines represent the snow thickness simulations with none redistribution, bulk redistribution, and snwITDrdg redistribution, respectively.

We assess the impact of the snow redistribution parameterization by comparing three Icepack configurations: no redistribution (none), bulk redistribution (bulk), and blowing-snow redistribution (snwITDrdg). All snow thickness values are converted to snow water equivalent for consistency with observations. Figure 1d shows that observed snow SWE increased from ~55 mm in December 2019 to ~65 mm by March 2020, then slightly decreased in April, peaked at 70 mm in May, and rapidly melted as temperatures rose (Figure 1a), with complete melt by July. The observed ice thickness increased from about 1.0 m in December 2019 to a maximum of about 1.9 m in early June, followed by rapid summer melt, decreasing to ~1.3 m by the end of July (Figure 1e).

For the none scheme, simulated SWE is overestimated relative to observations starting in mid-January, particularly during periods of snowfall. The simulation peaks at 155 mm on May 13 and then rapidly melts, with complete melt occurring by June 17. The bulk scheme reduces snow thickness slightly, but the seasonal trend remains similar. In contrast, the snwITDrdg scheme significantly reduces SWE, particularly during high-wind periods. When wind speed exceeds ~3.5 m/s (Figure 1b), snow particles are suspended and redistributed or deposited into open leads, reducing surface accumulation. Despite incorporating wind slab formation to limit snow suspension, frequent high winds drive continuous snow redistribution, improving agreement with observations. However, even with blowing-snow redistribution, simulated snow thickness remains overestimated in winter and spring and melts too rapidly in summer (Figure 1d). Compared with the snow thickness simulations, the ice thickness simulations show better agreement with the observations. The spread in simulated ice thickness among experiments is much smaller than the spread in snow

https://doi.org/10.5194/egusphere-2026-2179
Preprint. Discussion started: 2 June 2026

thickness. The none and bulk experiments slightly underestimate ice thickness during April to mid-June, while the snwITDrdg experiment exhibits a modest overestimation during this period. After mid-June, all simulations tend to underestimate the observed ice thickness. This bias is likely attributable to the rapid melt of simulated snow thickness during summer, which leads to increased exposure of sea ice to the warm atmosphere (Figure 1e).

3.2 Optimization of the Snow Redistribution Parameterization

We conduct a series of parameter optimization experiments aimed at improving the performance of the bulk and snwITDrdg snow redistribution schemes. Specifically, we focus on optimizing the ratio of snow mass on ridges to that on level ice (P) in the bulk redistribution scheme, as well as the sea ice concentration and the tuning coefficient γ in the snwITDrdg redistribution scheme.

In the bulk redistribution scheme, P is set to 0.3 based on estimates from SHEBA observations conducted two decades ago, which suggest that snow thickness on ice ridges is approximately 30% greater than that on level ice. However, observations during the MOSAiC campaign indicate that large ridges accumulated nearly five times the snow depth of level ice (Itkin et al., 2023). To quantify the sensitivity of the model to this parameter, we conducted a series of sensitivity experiments in which P was increased from 0.3 to 4.0 to examine its impact on simulated snow and ice thickness. The mean absolute error (MAE; $MAE = (1/n) \sum |HS\_sim - HS\_obs|$), where n is the number of data points over the period prior to June. HS_sim and HS_obs denote the simulated and observed snow and ice thickness, respectively, was used as the evaluation metric. The results show that increasing P leads to more snow being redistributed into open leads, thereby reducing the simulated snow thickness (Figure 2a). The minimum snow thickness MAE (~6.2 mm) is achieved when P = 4 (hereafter referred to as bulkm, Figure 3b).

https://doi.org/10.5194/egusphere-2026-2179
Preprint. Discussion started: 2 June 2026

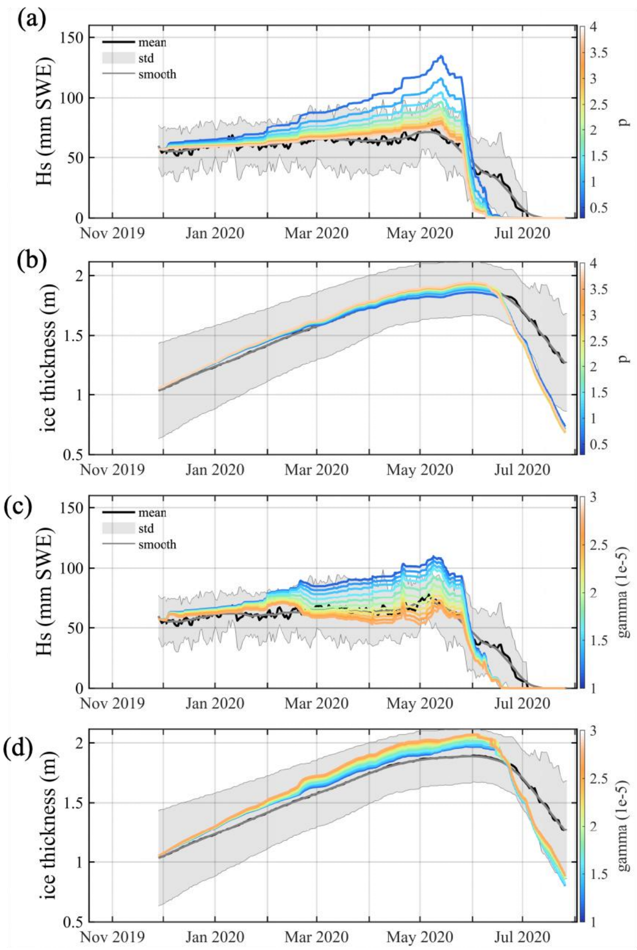

Figure 2. Time series of (a) snow thickness and (b) ice thickness from sensitivity experiments under the bulk redistribution scheme with varying P, and (c) snow thickness and (d) ice thickness from sensitivity experiments under the snwITDrdg scheme with varying γ. In panels (a) and (b), the 10 colored lines represent sensitivity experiments with P ranging from 0.3 to 4.0. In panels (c) and (d), the 11 colored lines correspond to sensitivity experiments with the γ tuning coefficient ranging from 1×10^{-5} to 3×10^{-5} .

In the snwITDrdg redistribution simulation, an increase in γ enhances the number of suspended snow particles, while a decrease in sea ice concentration enlarges the leads, which provide more open-water area to receive drifting snow. As a result, more snow particles are transported and deposited into these leads. There is a significant bias

https://doi.org/10.5194/egusphere-2026-2179
Preprint. Discussion started: 2 June 2026

between the simulated and observed sea ice concentration (Figure 3a). The simulated sea ice concentration gradually decreased from 0.98 to 0.92 by the end of July, after which it decreases rapidly. The observed sea ice concentration experiences significant reductions both at the end of April and July, reaching as low as 0.7. This increases leads, thereby increasing the amount of snow blown into the leads during the snwITDrdg redistribution. γ is a tuning coefficient for the erosion rate, with a default value of 1×10^{-5}. We conducted 11 sensitivity experiments, varying the γ value from 1×10^{-5} to 3×10^{-5}, which increased the snow erosion rate and consequently reduced the simulated snow thickness. It should be noted that γ cannot be uniquely constrained by snow depth observations alone, because its influence is strongly coupled with uncertainties in snow density (observations: 250-400 kg m^{-3}; model value: 330 kg m^{-3}) and the subgrid-scale ice thickness distribution (σITD; observations: 0.03-0.8 m; model range: 0.4-0.8 m). Therefore, in this study, γ is interpreted as an effective parameter within the default Icepack configuration rather than as a physically universal constant. Furthermore, using isotope-based observations from the MOSAiC expedition, Clemens-Sewall et al. (2023) found that snow fall into a lead during warmer and windier events with prolonged lead openings (19–28 April 2020) corresponded to an accumulated snow loss of approximately 7–11 mm of snow water equivalent per lead area. These observations were also used to evaluate the simulations (Figure 3b).

When the snow thickness simulation is conducted without prescribing sea ice concentration, adjusting the γ coefficient does not result in accumulated snow loss to leads within the 7-11 mm range (Figure 3b). However, when the AMSR2 sea ice concentration is prescribed in the snow thickness simulation, adjusting the γ coefficient between 1.6×10^{-5} and 2.4×10^{-5} yields accumulated snow loss to leads within the 7–11 mm per lead area range. When γ is set to 2.4×10^{-5} (hereafter referred to as snwITDrdgm), the simulated snow thickness generally agrees well with the observations, resulting in a minimum MAE of 6.4 mm, with slight overestimations in

https://doi.org/10.5194/egusphere-2026-2179
Preprint. Discussion started: 2 June 2026

February and May, and continued rapid melting in June compared to the observations (Figure 2b).

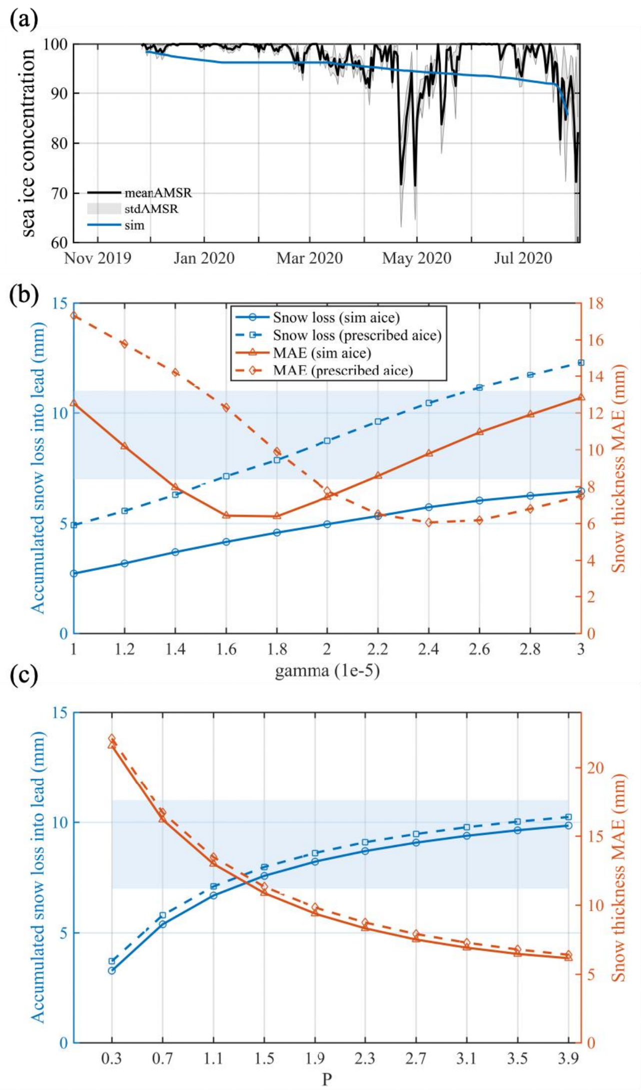

Figure 3. (a) Time series of sea ice concentration from AMSR2 observations and Icepack simulations. (b) and (c) show the statistical results for sensitivity experiments varying the γ and P parameters, respectively. The blue line and the left blue y-axis represent the accumulated snow loss into open leads during the period from 9 April to 28 April, while the orange line and the right orange y-axis indicate the mean absolute

https://doi.org/10.5194/egusphere-2026-2179
Preprint. Discussion started: 2 June 2026

error (MAE, in mm) between simulated and observed snow thickness. The blue shaded area denotes the observed range of accumulated snow loss into open leads (~7–11 mm per lead area) based on Clemens-Sewall et al. (2023). Solid lines denote simulations without prescribed observed sea ice concentration, whereas dashed lines denote simulations with prescribed observed sea ice concentration.

In the snow mass balance, snow thickness is influenced by snowfall (Sf), snowmelt (Sm), snow sublimation (Ssu), snow-ice formation (Si), and snow loss into open leads (Slo). This study investigates the impact of different snow redistribution schemes, with and without prescribing sea ice concentration, on the snow mass balance. The results (Figure 4) show that, compared to the none scheme, the bulk scheme increases the amount of snow entering the leads by reducing the snowfall reaching the ice layer. Additionally, compared to the bulk scheme, the snwITDrdg scheme leads to increased snow-ice formation. In addition to depositing a portion of snow particles into open leads, the snwITDrdg scheme diagnostically redistributes snow among ice thickness categories. This redistribution, modulated by the ridged-ice fraction and surface type within each category, results in increased snow thickness over thinner ice categories, making the ice more susceptible to surface flooding and subsequent snow-ice formation. Compared to the bulk scheme, the bulkm scheme removes a larger fraction of precipitation, resulting in reduced overall snow accumulation. Meanwhile, the snwITDrdgm scheme increases Slo relative to snwITDrdg, thereby reducing snowmelt at the end of the simulation. The Ssu values are relatively consistent across all snow redistribution schemes. Prescribing sea ice concentration has minimal effect on the none and bulk schemes. However, within the snwITDrdg and snwITDrdgm scheme, prescribing sea ice concentration leads to a significant reduction in Slo and a corresponding increase in Sm.

https://doi.org/10.5194/egusphere-2026-2179
Preprint. Discussion started: 2 June 2026

329

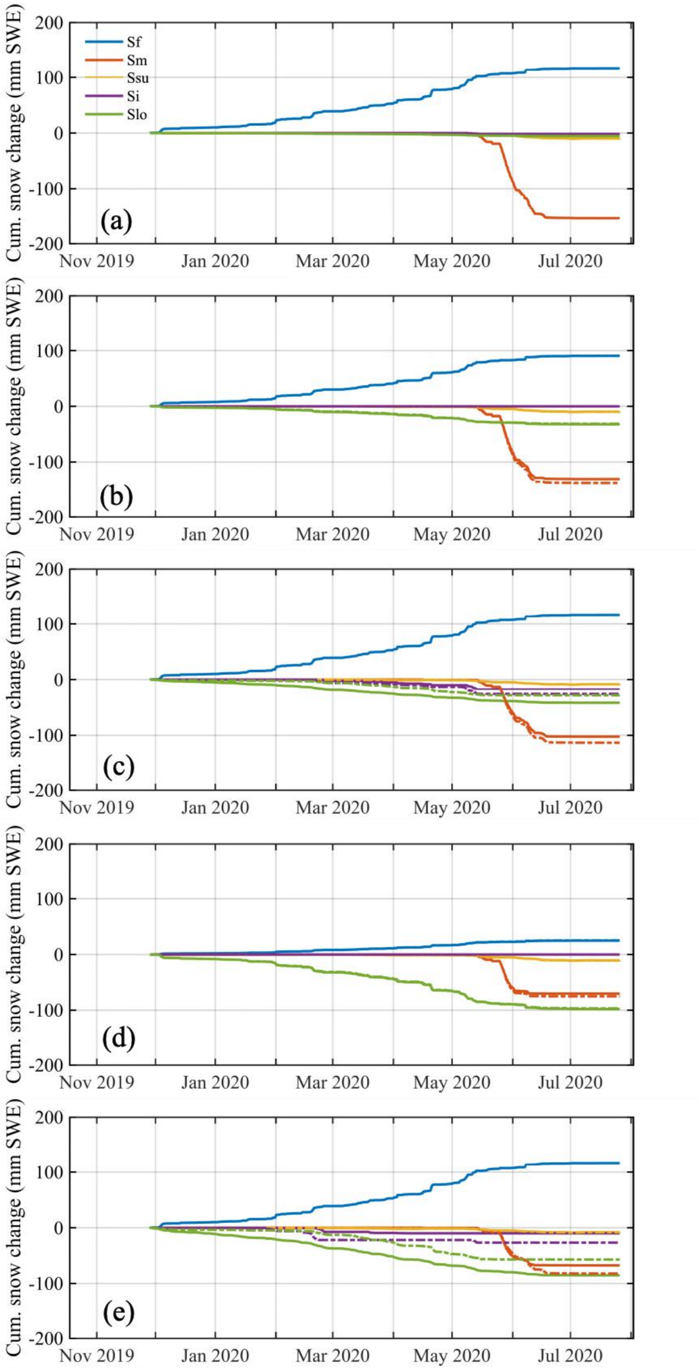

330 Figure 4. Time series of cumulative snow changes in (a) none, (b) bulk, (c)

snwITDrdg, (d) bulkm and (e) snwITDrdgm redistribution schemes. Different colored lines represent snowfall (Sf), snowmelt (Sm), snow sublimation (Ssu), snow-ice formation (Si), and snow loss into open leads (Slo), respectively. Solid lines denote simulations without prescribed AMSR2 sea ice concentration, while dashed lines indicate simulations with prescribed AMSR2 sea ice concentration.

4. Conclusions and Discussions

Snow plays a vital role in sea ice thermodynamics, yet snow accumulation remains a key uncertainty in sea ice modeling. Using the Icepack column model, we simulated snow thickness during the MOSAiC campaign under various snow redistribution schemes, and further explored both bulk and snwITDrdg parameterization to enhance the agreement with observations. Our results show that without snow redistribution, simulated snow thickness is significantly overestimated in winter and spring, resulting in a delayed seasonal peak and an earlier snow melt in summer. The bulk redistribution scheme slightly reduces snow accumulation while showing a modest improvement in seasonal timing. The snwITDrdg redistribution scheme further reduces snow thickness, though biases persist, especially during snowfall events.

To address this issue, we conducted sensitivity experiments for both snow redistribution schemes. In the bulk scheme, we varied the parameter P from 0.3 to 4 based on MOSAiC observations. When P = 4, the simulated snow thickness shows the best agreement with observations, with a mean absolute error (MAE) of 6.2 mm. In the snwITDrdg scheme, given the large observational uncertainties in snow density and subgrid-scale ice thickness distribution (ITD), the coefficient γ is treated as an effective tuning parameter that accounts for unresolved uncertainties in snow physical properties and ice thickness heterogeneity. We varied γ from 1×10^{-5} to 3×10^{-5}, with and without prescribing AMSR2 sea ice concentration. When sea ice concentration is not prescribed, adjusting γ does not lead to accumulated snow loss to leads within

https://doi.org/10.5194/egusphere-2026-2179
Preprint. Discussion started: 2 June 2026

the observed range of 7-11 mm per lead area. In contrast, when AMSR2 sea ice concentration is prescribed, the simulated accumulated snow loss to leads falls within the observed range. Specifically, when $\gamma = 2.4\times10^{-5}$, the simulated snow thickness generally agrees well with observations, yielding a mean absolute error of 6.4 mm. These results indicate that the parameter P in the bulk scheme and the effective tuning coefficient γ in the snwITDrdg scheme both have a significant influence on simulated snow thickness. Moreover, accurate sea ice concentration is crucial for realistic snow thickness simulations in the snwITDrdg scheme.

Despite improvements, several limitations remain. The simulated snow thickness still peaks approximately seven days later than observed and melts too quickly in summer. This discrepancy likely stems from uncertainties in snowfall datasets. For example, the PWD–ERA5 average shows increased snowfall between May 6 and 13 (Figure 1c), while observed snow thickness declined, suggesting potential errors in observations or reanalysis (Wagner et al., 2022). Rapid summer melt may also result from missing melt-pond physics or inaccurate snow thermal conductivity, leading to excessive surface heat fluxes (Yin et al., 2021). In addition, Icepack estimates a constant snow density of 330 kg m^{-3}, whereas actual snow density evolves with wind compaction, temperature fluctuations, moisture content, and sublimation (Liston et al., 2020; Macfarlane et al., 2023), contributing to mass and thickness biases. The treatment of suspended snow particles is simplified in Icepack: all excess snow is assumed to enter leads. While sublimation of suspended snow represents an important loss pathway in the Arctic (Liston et al., 2020), the distinction between atmospheric and oceanic loss pathways does not affect the results of this study. Although the representativeness of the MOSAiC observations should be considered, they constitute one of the most comprehensive datasets for examining snow and sea ice processes in the central Arctic. The findings of this study provide new insights into snow thickness simulation and the parameterization of snow redistribution, contributing to improved modeling of

https://doi.org/10.5194/egusphere-2026-2179
Preprint. Discussion started: 2 June 2026

Arctic snow conditions.

Data availability

The MOSAiC meteorological data are available from the Arctic Data Center (Cox et al., 2021a, 2021b, 2021c, 2023). SIMBA ice and snow thickness data are available from PANGAEA (Lei et al., 2021). Autonomous sea ice measurements (Ocean CTD Buoy and Flux Buoy) from 1 October 2019 to 1 September 2020 were obtained from the Sea Ice Portal (Grosfeld et al., 2016). AMSR2 ASI sea ice concentration data were obtained from the University of Bremen Sea Ice Portal and are calculated following Spreen et al. (2008). SAR-based sea ice divergence data drift during MOSAiC 2019/2020 are available from PANGAEA (von Albedyll, 2024)

Competing interests

At least one of the (co-)authors is a member of the editorial board of The Cryosphere

Author contributions

JL, CL and FG conceptualized this study and designed the numerical experiments. FG carried out the numerical experiments and wrote the manuscript. CL, BH, QY and JL helped analyze the results and revised the manuscript.

Acknowledgments

The authors would like to thank all persons involved in the international Multidisciplinary drifting Observatory for the Study of Arctic Climate (MOSAiC) expedition. We acknowledge the University of Colorado/NOAA surface flux team for the effort in collecting and post-processing the meteorological measurements. We

https://doi.org/10.5194/egusphere-2026-2179
Preprint. Discussion started: 2 June 2026

appreciate the Polar Research Institute of China for the efforts in obtaining ice thickness and snow thickness data from the SIMBA buoys. The buoy data from 1 October 2019 to 1 September 2020 were obtained from https://www.meereisportal.de (funding: REKLIM-2013-04). AMSR2 ASI sea ice concentration data were provided by the Institute of Environmental Physics, University of Bremen. We are grateful to CICE Consortium for sharing Icepack and its documentation (https://github.com/CICE-Consortium/Icepack).

Financial support

This research is supported by the National Key R&D Program of China (2022YFE0106300), the National Natural Science Foundation of China (42506245).

References

Bitz, C. M.: Description of initial conditions and forcing data for the SHEBA single column model runs, University of Washington, available at https://atmos.washington.edu/~bitz/column_model/notes_forcing_data, accessed 16 January 2026.

Bliss, A. C., Hutchings, J. K., and Watkins, D. M.: Sea ice drift tracks from autonomous buoys in the MOSAiC Distributed Network, Scientific Data, 10, 403, 10.1038/s41597-023-02311-y, 2023.

Callaghan, T. V., Johansson, M., Brown, R. D., Groisman, P. Ya., Labba, N., Radionov, V., Barry, R. G., Bulygina, O. N., Essery, R. L. H., Frolov, D. M., Golubev, V. N., Grenfell, T. C., Petrushina, M. N., Razuvaev, V. N., Robinson, D. A., Romanov, P., Shindell, D., Shmakin, A. B., Sokratov, S. A., Warren, S., and Yang, D.: The Changing Face of Arctic Snow Cover: A Synthesis of Observed and Projected

https://doi.org/10.5194/egusphere-2026-2179
Preprint. Discussion started: 2 June 2026

Changes, AMBIO, 40, 17-31, https://doi.org/10.1007/s13280-011-0212-y, 2011.

Cox, C., Gallagher, M., Shupe, M., Persson, O., Solomon, A., Ayers, T., Costa, D., Hutchings, J., Leach, J., Morris, S., Osborn, J., Pezoa, S., and Uttal, T.: Atmospheric Surface Flux Station #30 measurements (Level 1 Raw), Multidisciplinary Drifting Observatory for the Study of Arctic Climate (MOSAiC), central Arctic, October 2019 - September 2020, Arctic Data Center, https://doi.org/doi:10.18739/A20C4SM1J, 2021a.

Cox, C., Gallagher, M., Shupe, M., Persson, O., Solomon, A., Ayers, T., Costa, D., Hutchings, J., Leach, J., Morris, S., Osborn, J., Pezoa, S., and Uttal, T.: Atmospheric Surface Flux Station #40 measurements (Level 1 Raw), Multidisciplinary Drifting Observatory for the Study of Arctic Climate (MOSAiC), central Arctic, October 2019 - September 2020, Arctic Data Center, https://doi.org/doi:10.18739/A2CJ87M7G, 2021b.

Cox, C., Gallagher, M., Shupe, M., Persson, O., Solomon, A., Ayers, T., Costa, D., Hutchings, J., Leach, J., Morris, S., Osborn, J., Pezoa, S., and Uttal, T.: Atmospheric Surface Flux Station #50 measurements (Level 1 Raw), Multidisciplinary Drifting Observatory for the Study of Arctic Climate (MOSAiC), central Arctic, October 2019 - September 2020, Arctic Data Center, https://doi.org/doi:10.18739/A2445HD46, 2021c.

Cox, C., Gallagher, M., Shupe, M., Persson, O., Blomquist, B., Grachev, A., Riihimaki, L., Kutchenreiter, M., Morris, V., Solomon, A., Brooks, I., Costa, D., Gottas, D., Hutchings, J., Osborn, J., Morris, S., Preusser, A., and Uttal, T.: Met City meteorological and surface flux measurements (Level 3 Final), Multidisciplinary Drifting Observatory for the Study of Arctic Climate (MOSAiC), central Arctic, October 2019 - September 2020., Arctic Data Center, https://doi.org/doi:10.18739/A2PV6B83F, 2023.

https://doi.org/10.5194/egusphere-2026-2179
Preprint. Discussion started: 2 June 2026

Cheng, B., Launiainen, J., and Vihma, T.: Modelling of Superimposed Ice Formation and SubSurface Melting in the Baltic Sea, Geophysica, 39, 31-50, 2003.

Clemens-Sewall, D., Smith, M. M., Holland, M. M., Polashenski, C., and Perovich, D.: Snow redistribution onto young sea ice: Observations and implications for climate models, Elementa: Science of the Anthropocene, 10, 00115, 10.1525/elementa.2021.00115, 2022.

Clemens-Sewall, D., Polashenski, C., Frey, M. M., Cox, C. J., Granskog, M. A., Macfarlane, A. R., Fons, S. W., Schmale, J., Hutchings, J. K., von Albedyll, L., Arndt, S., Schneebeli, M., and Perovich, D.: Snow Loss Into Leads in Arctic Sea Ice: Minimal in Typical Wintertime Conditions, but High During a Warm and Windy Snowfall Event, Geophysical Research Letters, 50, e2023GL102816, https://doi.org/10.1029/2023GL102816, 2023.

Déry, S. J., and Yau, M. K.: Large-scale mass balance effects of blowing snow and surface sublimation, Journal of Geophysical Research: Atmospheres, 107, ACL 8-1-ACL 8-17, 10.1029/2001JD001251, 2002.

Eicken, H., Grenfell, T. C., Perovich, D. K., Richter-Menge, J. A., and Frey, K.: Hydraulic controls of summer Arctic pack ice albedo, Journal of Geophysical Research: Oceans, 109, 10.1029/2003JC001989, 2004.

Gu, F., Kauker, F., Yang, Q., Han, B., Fang, Y., and Liu, C.: Effects of Freezing Temperature Parameterization on Simulated Sea-Ice Thickness Validated by MOSAiC Observations, Geophysical Research Letters, 51, e2024GL108281, 10.1029/2024GL108281, 2024.

Granskog, M. A., Rösel, A., Dodd, P. A., Divine, D., Gerland, S., Martma, T., and Leng, M. J.: Snow contribution to first-year and second-year Arctic sea ice mass balance north of Svalbard, Journal of Geophysical Research: Oceans, 122, 2539-2549, 10.1002/2016JC012398, 2017.

R., Hendricks, S., Hiller, W., Heygster, G., Krumpen, T., Lemke, P., Melsheimer, C., Nicolaus, M., Ricker, R., and Weigelt, M.: Online sea-ice knowledge and data platform, Polarforschung, Bremerhaven: Alfred Wegener Institute for Polar and Marine Research & German Society of Polar Research, 10.2312/polfor.2016.011, 2016.

Hao, G., Shen, H., and Sun, Y.: Simulation and analysis of the snow blowing on landfast sea ice, Antarctica, Acta Oceanologica Sinica, 44, 161-171, 10.1007/s13131-025-2464-6, 2025.

Hunke, E., Allard, R., Bailey, D. A., Blain, P., Craig, T., Dupont, F., DuVivier, A., Grumbine, R., Hebert, D., Holland, M., Jeffery, N., Lemieux, J.-F., Rasmussen, T., Ribergaard, M., and Roberts, A.: CICE-Consortium/Icepack: Icepack1.3.2. doi:10.5281/zenodo.6967671, 2022.

Itkin, P., Hendricks, S., Webster, M., von Albedyll, L., Arndt, S., Divine, D., Jaggi, M., Oggier, M., Raphael, I., Ricker, R., Rohde, J., Schneebeli, M., and Liston, G. E.: Sea ice and snow characteristics from year-long transects at the MOSAiC Central Observatory, Elementa: Science of the Anthropocene, 11, 00048, https://doi.org/10.1525/elementa.2022.00048, 2023.

Jeffries, M. O., Krouse, H. R., Hurst-Cushing, B., and Maksym, T.: Snow-ice accretion and snow-cover depletion on Antarctic first-year sea-ice floes, Annals of Glaciology, 33, 51-60, 10.3189/172756401781818266, 2001.

Kwok, R.: Arctic sea ice thickness, volume, and multiyear ice coverage: losses and coupled variability (1958-2018), Environmental Research Letters, 13, 105005,

https://doi.org/10.5194/egusphere-2026-2179
Preprint. Discussion started: 2 June 2026

10.1088/1748-9326/aae3ec, 2018.

Lecomte, O., Fichefet, T., Vancoppenolle, M., Domine, F., Massonnet, F., Mathiot, P., Morin, S., and Barriat, P. Y.: On the formulation of snow thermal conductivity in large-scale sea ice models, Journal of Advances in Modeling Earth Systems, 5, 542-557, https://doi.org/10.1002/jame.20039, 2013.

Lecomte, O., Fichefet, T., Flocco, D., Schroeder, D., and Vancoppenolle, M.: Interactions between wind-blown snow redistribution and melt ponds in a coupled ocean-sea ice model, Ocean Modelling, 87, 67-80, 10.1016/j.ocemod.2014.12.003, 2015.

Lei, R., Cheng, B., Heil, P., Vihma, T., Wang, J., Ji, Q., and Zhang, Z.: Seasonal and interannual variations of sea ice mass balance from the Central Arctic to the Greenland Sea, Journal of Geophysical Research: Oceans, 123, 2422-2439, 2018.

Lei, R., Cheng, B., and Hoppmann, M.: Snow depth and sea ice thickness derived from the measurements of SIMBA buoys deployed in the Arctic Ocean during the Legs 1a, 1, and 3 of the MOSAiC campaign in 2019-2020, PANGAEA, 10.1594/PANGAEA.938244, 2021.

Lei, R., Cheng, B., Hoppmann, M., Zhang, F., Zuo, G., Hutchings, J. K., Lin, L., Lan, M., Wang, H., Regnery, J., Krumpen, T., Haapala, J., Rabe, B., Perovich, D. K., and Nicolaus, M.: Seasonality and timing of sea ice mass balance and heat fluxes in the Arctic transpolar drift during 2019 − 2020, Elementa: Science of the Anthropocene, 10, 000089, https://doi.org/10.1525/elementa.2021.000089, 2022.

Leonard, K. C., and Maksym, T.: The importance of wind-blown snow redistribution to snow accumulation on Bellingshausen Sea ice, Annals of Glaciology, 52, 271-278, 10.3189/172756411795931651, 2011.

https://doi.org/10.5194/egusphere-2026-2179
Preprint. Discussion started: 2 June 2026

Leppäranta, M.: A Growth Model for Black Ice, Snow Ice and Snow Thickness in Subarctic Basins, Hydrology Research, 14, 59-70, 10.2166/nh.1983.0006, 1983.

Liston, G. E., Itkin, P., Stroeve, J., Tschudi, M., Stewart, J. S., Pedersen, S. H., Reinking, A. K., and Elder, K.: A Lagrangian Snow-Evolution System for Sea-Ice Applications (SnowModel-LG): Part I—Model Description, Journal of Geophysical Research: Oceans, 125, e2019JC015913, https://doi.org/10.1029/2019JC015913, 2020.

Luo, L., and Zhang, J.: Blowing Snow Contributes to Positive Surface Energy Budget and Negative Surface Mass Balance During a Melting Season of Larsen C Ice Shelf, Antarctic Peninsula, Geophysical Research Letters, 49, e2022GL098864, 10.1029/2022GL098864, 2022.

Macfarlane, A., Schneebeli, M., Dadic, R., Tavri, A., Immerz, A., Polashenski, C., Krampe, D., Clemens-Sewall, D., Wagner, D., Perovich, D., Hannula, H.-R., Raphael, I., Matero, I., Regnery, J., Smith, M., Nicolaus, M., Jaggi, M., Oggier, M., Webster, M., and Fons, S.: A Database of Snow on Sea Ice in the Central Arctic Collected during the MOSAiC expedition, Scientific Data, 10, https://doi.org/10.1038/s41597-023-02273-1, 2023.

Maksym, T., and Jeffries, M. O.: A one-dimensional percolation model of flooding and snow ice formation on Antarctic sea ice, Journal of Geophysical Research: Oceans, 105, 26313-26331, 10.1029/2000JC900130, 2000.

Massom, R. A., Eicken, H., Hass, C., Jeffries, M. O., Drinkwater, M. R., Sturm, M., Worby, A. P., Wu, X., Lytle, V. I., Ushio, S., Morris, K., Reid, P. A., Warren, S. G., and Allison, I.: Snow on Antarctic sea ice, Reviews of Geophysics, 39, 413 − 445, https://doi.org/10.1029/2000RG000085, 2001.

https://doi.org/10.5194/egusphere-2026-2179
Preprint. Discussion started: 2 June 2026

Maykut, G. A., and Untersteiner, N.: Some results from a time-dependent thermodynamic model of sea ice, Journal of Geophysical Research, 76, 1550-1575, 10.1029/JC076i006p01550, 1971.

Merkouriadi, I., Cheng, B., Graham, R. M., Rösel, A., and Granskog, M. A.: Critical Role of Snow on Sea Ice Growth in the Atlantic Sector of the Arctic Ocean, Geophysical Research Letters, 44, 10479-10485, 10.1002/2017GL075494, 2017.

Merkouriadi, I., Liston, G. E., Graham, R. M., and Granskog, M. A.: Quantifying the Potential for Snow-Ice Formation in the Arctic Ocean, Geophysical Research Letters, 47, e2019GL085020, 10.1029/2019GL085020, 2020.

Perovich, D. K., Grenfell, T. C., Light, B., and Hobbs, P. V.: Seasonal evolution of the albedo of multiyear Arctic sea ice, Journal of Geophysical Research: Oceans, 107, SHE 20-1-SHE 20-13, 10.1029/2000JC000438, 2002.

Petty, A. A., Webster, M., Boisvert, L., and Markus, T.: The NASA Eulerian Snow on Sea Ice Model (NESOSIM) v1.0: initial model development and analysis, Geoscientific Model Development, 11, 4577-4602, 10.5194/gmd-11-4577-2018, 2018.

Polashenski, C., Perovich, D., and Courville, Z.: The mechanisms of sea ice melt pond formation and evolution, Journal of Geophysical Research: Oceans, 117, 2011JC007231, 10.1029/2011JC007231, 2012.

Rabe, B., Heuzé, C., Regnery, J., Aksenov, Y., Allerholt, J., Athanase, M., Bai, Y., Basque, C., Bauch, D., Baumann, T. M., Chen, D., Cole, S. T., Craw, L., Davies, A., Damm, E., Dethloff, K., Divine, D. V., Doglioni, F., Ebert, F., Fang, Y.-C., Fer, I., Fong, A. A., Gradinger, R., Granskog, M. A., Graupner, R., Haas, C., He, H., He, Y., Hoppmann, M., Janout, M., Kadko, D., Kanzow, T., Karam, S., Kawaguchi, Y.,

https://doi.org/10.5194/egusphere-2026-2179
Preprint. Discussion started: 2 June 2026

Koenig, Z., Kong, B., Krishfield, R. A., Krumpen, T., Kuhlmey, D., Kuznetsov, I., Lan, M., Laukert, G., Lei, R., Li, T., Torres-Valdés, S., Lin, L., Lin, L., Liu, H., Liu, N., Loose, B., Ma, X., McKay, R., Mallet, M., Mallett, R. D. C., Maslowski, W., Mertens, C., Mohrholz, V., Muilwijk, M., Nicolaus, M., O'Brien, J. K., Perovich, D., Ren, J., Rex, M., Ribeiro, N., Rinke, A., Schaffer, J., Schuffenhauer, I., Schulz, K., Shupe, M. D., Shaw, W., Sokolov, V., Sommerfeld, A., Spreen, G., Stanton, T., Stephens, M., Su, J., Sukhikh, N., Sundfjord, A., Thomisch, K., Tippenhauer, S., Toole, J. M., Vredenborg, M., Walter, M., Wang, H., Wang, L., Wang, Y., Wendisch, M., Zhao, J., Zhou, M., and Zhu, J.: Overview of the MOSAiC expedition: Physical oceanography, Elementa: Science of the Anthropocene, 10, 00062, https://doi.org/10.1525/elementa.2021.00062, 2022.

Schmidt, R. A.: Vertical profiles of wind speed, snow concentration, and humidity in blowing snow, Boundary-Layer Meteorology, 23, 223-246, 10.1007/BF00123299, 1982.

Ruti, P. M., Marullo, S., D'Ortenzio, F., and Tremant, M.: Comparison of analyzed and measured wind speeds in the perspective of oceanic simulations over the Mediterranean basin: Analyses, QuikSCAT and buoy data, Journal of Marine Systems, 70, 33-48, 10.1016/j.jmarsys.2007.02.026, 2008.

Shupe, M. D., Rex, M., Blomquist, B., Persson, P. O. G., Schmale, J., Uttal, T., Althausen, D., Angot, H., Archer, S., Bariteau, L., Beck, I., Bilberry, J., Bucci, S., Buck, C., Boyer, M., Brasseur, Z., Brooks, I. M., Calmer, R., Cassano, J., Castro, V., Chu, D., Costa, D., Cox, C. J., Creamean, J., Crewell, S., Dahlke, S., Damm, E., de Boer, G., Deckelmann, H., Dethloff, K., Dütsch, M., Ebell, K., Ehrlich, A., Ellis, J., Engelmann, R., Fong, A. A., Frey, M. M., Gallagher, M. R., Ganzeveld, L., Gradinger, R., Graeser, J., Greenamyer, V., Griesche, H., Griffiths, S., Hamilton, J., Heinemann, G., Helmig, D., Herber, A., Heuzé, C., Hofer, J., Houchens, T., Howard, D., Inoue, J., Jacobi, H.-W., Jaiser, R., Jokinen, T., Jourdan, O., Jozef, G., King, W., Kirchgaessner, A., Klingebiel, M., Krassovski, M., Krumpen, T., Lampert, A., Landing, W., Laurila, T., Lawrence, D., Lonardi, M., Loose, B., Lüpkes, C., Maahn, M., Macke, A., Maslowski, W., Marsay, C., Maturilli, M., Mech, M., Morris, S., Moser, M., Nicolaus, M., Ortega, P., Osborn, J., Pätzold, F., Perovich, D. K., Petäjä, T., Pilz, C., Pirazzini, R., Posman, K., Powers, H., Pratt, K. A., Preußer, A., Quéléver, L., Radenz, M., Rabe, B., Rinke, A., Sachs, T., Schulz, A., Siebert, H., Silva, T., Solomon, A., et al.: Overview of the MOSAiC expedition: Atmosphere, Elementa: Science of the Anthropocene, 10, 00060, https://doi.org/10.1525/elementa.2021.00060, 2022.

Spreen, G., Kaleschke, L., and Heygster, G.: Sea ice remote sensing using AMSR-E 89-GHz channels, Journal of Geophysical Research: Oceans, 113, 10.1029/2005JC003384, 2008.

Sturm, M., Holmgren, J., and Perovich, D. K.: Winter snow cover on the sea ice of the Arctic Ocean at the Surface Heat Budget of the Arctic Ocean (SHEBA): Temporal evolution and spatial variability, Journal of Geophysical Research: Oceans, 107, SHE 23-1-SHE 23-17, 10.1029/2000JC000400, 2002.

Van den Broeke, M. R., Reijmer, C. H., and Van De Wal, R. S.: A study of the surface mass balance in Dronning Maud Land, Antarctica, using automatic weather stations, Journal of Glaciology, 50, 565-582, 2004.

von Albedyll, L.: Sea ice lead fractions from SAR-derived sea ice divergence in the Transpolar Drift during MOSAiC 2019/2020 [Dataset], PANGAEA, 10.1594/PANGAEA.963671, 2024.

Wagner, D. N., Shupe, M. D., Cox, C., Persson, O. G., Uttal, T., Frey, M. M., Kirchgaessner, A., Schneebeli, M., Jaggi, M., Macfarlane, A. R., Itkin, P., Arndt, S., Hendricks, S., Krampe, D., Nicolaus, M., Ricker, R., Regnery, J., Kolabutin, N.,

https://doi.org/10.5194/egusphere-2026-2179
Preprint. Discussion started: 2 June 2026

Shimanshuck, E., Oggier, M., Raphael, I., Stroeve, J., and Lehning, M.: Snowfall and snow accumulation during the MOSAiC winter and spring seasons, The Cryosphere, 16, 2373 – 2402, https://doi.org/10.5194/tc-16-2373-2022, 2022.

Wang, C., Cheng, B., Wang, K., Gerland, S., and Pavlova, O.: Modelling snow ice and superimposed ice on landfast sea ice in Kongsfjorden, Svalbard, Polar Research, 34, 20828, 10.3402/polar.v34.20828, 2015.

Webster, M., Gerland, S., Holland, M., Hunke, E., Kwok, R., Lecomte, O., Massom, R., Perovich, D., and Sturm, M.: Snow in the changing sea-ice systems, Nature Clim Change, 8, 946 – 953, https://doi.org/10.1038/s41558-018-0286-7, 2018.

Yin, H., Su, J., and Cheng, B.: The effect of snow density evolution on modelled snow depth in the Arctic, Haiyang Xuebao, 43, 15, 2021.

Zhao, J., Lu, Y., Zhao, H., Wang, X., and Liu, J.: Influence of Snow Redistribution and Melt Pond Schemes on Simulated Sea Ice Thickness During the MOSAiC Expedition, Journal of Marine Science and Engineering, 13, 1317, 10.3390/jmse13071317, 2025.